ELSEVIER

Biochemical Pharmacology 63 (2002) 797–807

Biochemical Pharmacology

Regulation of cyclic AMP in rat pulmonary microvascular endothelial cells by rolipram-sensitive cyclic AMP phosphodiesterase (PDE4)

W. Joseph Thompson*, Takashi Ashikaga[1], John J. Kelly[2], Li Liu[3], Bing Zhu, Lakshimi Vemavarapu, Samuel J. Strada

Department of Pharmacology, University of South Alabama College of Medicine, Mobile, AL 36608, USA

Received 8 June 2000; accepted 6 July 2001

Abstract

We report here studies on the regulation of the metabolism of adenosine 3′,5′-monophosphate (cAMP) in established and primary cultures of rat pulmonary microvascular endothelial cells (RPMVEC). Inhibition by rolipram, a selective inhibitor of cAMP phosphodiesterase (PDE) of the PDE4 gene family, was required to achieve maximal cAMP accumulation induced by direct or receptor-mediated adenylate cyclase activation when measured by [^{3}H]-adenine prelabeling. Rolipram increased cAMP accumulation more effectively than did forskolin, isoproterenol, or adenosine derivatives alone, although extensive synergy was seen with combined agents. High-affinity PDE4 inhibitors, but not low-affinity or non-selective inhibitors, were effective inducers of cAMP accumulation in intact cells. The maximum effects (i.e. intrinsic activities) of these agents in the intact cell did not correlate with their *in vitro* PDE4 inhibitory affinities. RPMVEC were shown to express almost exclusively the PDE4 gene family isoforms A6 and B3. Guanosine 3′,5′-monophosphate hydrolysis, observed in other types of endothelial cells was not found in early or late passage RPMVEC. Reverse transcription-polymerase chain reaction identification of mRNAse supported these conclusions with the exception that PDE2 and PDE4D mRNA isoform transcripts were present. These studies also support the conclusion that the mechanism of rolipram reversal of rat lung ischemia-reperfusion-induced permeability involves PDE4 inhibition in the microvascular endothelial cells of the lung.

Keywords: Cyclic nucleotide phosphodiesterase; Cyclic AMP metabolism; Rolipram; Phosphodiesterease inhibitors; Endothelial cell permeability; Signal transduction

1. Introduction

Cyclic nucleotide phosphodiesterase(s) (CN PDEs) (EC 3.1.4.17) have a central role in the regulation of endothelial cell (EC) barrier permeability [1–6]. CN PDEs constitute a complex system of 11 gene families with multiple subfamilies that hydrolyze cAMP and guanosine 3′,5′-monophosphate (cGMP) [7,8]. Various inhibitors, selective for different PDE isozymes, have been shown to differentially affect tissue responses depending upon isoform expression [9,10]. For example, selective inhibitors of the PDE2 and PDE3 families of isozymes in the lung, but not inhibitors of PDE1, 4, or 5 enzymes, attenuate acute hypoxia-induced vasoconstriction [11,12]. Zaprinast, a relatively selective PDE5 inhibitor, reverses chronic pulmonary hypertension in rats [13]. Selective inhibitors of the PDE4 gene family isoforms consisting of subfamilies A–D have cell-specific actions [14,15] over other PDE inhibitors. Selective inhibition of PDE4 isoforms provides the basis for a new class

* Corresponding author. Present address: Cell Pathways Inc., 702 Electronic Drive, Horsham, PA 19044, USA. Tel.: +1-215-706-3803; fax: +1-215-706-3801.

E-mail address: jthompson@cellpathways.com (W.J. Thompson).

[1] Present address: 1st Department of Medicine, Yokuhama Minami Kyosai Hospital, 500 Mutsu-ura, Kanazawa-Ku, Yokoham-shi, Kanagawa-Ken 236, Japan.

[2] Present address: Protein Phosphorylation Laboratory, Imperial Cancer Research Fund, 44 Lincoln's Inn Fields, London WC2A 3PX, UK.

[3] Present address: Cell Pathways Inc., 702 Electronic Drive, Horsham, PA 19044, USA.

Abbreviations: CN PDE, cyclic nucleotide phosphodiesterase(s); PDE, phosphodiesterase; RPMVEC, rat pulmonary microvascular endothelial cells; COPD, chronic obstructive pulmonary disease; EC, endothelial cell; cGMP, guanosine 3′,5′-monophosphate; TCA, trichloroacetic acid; cAMP, adenosine 3′,5′-monophosphate; FBS, fetal bovine serum; CGS 21680, 2-*p*-(2-carboxyethyl)phenethylamino-5′-*N*-ethylcarboxamido adenosine; SQ65442, 1-ethyl-4-(ethylthio)-1*H*-pyrazolol[3,4-*b*]-pyridine-5-carboxylic acid, ethyl ester; RO 20-1724, 4-(3-butoxy-4-methoxy benzyl)-2-imidazolidinone; NECA, adenosine-5′-(*N*-ethylcarboxamide); RT-PCR, reverse transcription-polymerase chain reaction; DMEM, Dulbecco's minimal essential medium.

0006-2952/02/$ – see front matter
PII: S0006-2952(01)00914-5

of agents to treat chronic obstructive pulmonary disease (COPD) and asthma [9].

Decreased cAMP and increased calcium levels in some types of ECs have been associated with increased permeability in several studies [3,16–18]. Tumor necrosis factor α-induced permeability is associated with an activation of PDE4 and PDE2 and concomitant decreased cAMP levels in conduit vessel ECs [3]. Conversely, agents that increase EC cAMP levels are known to prevent barrier injury in several lung injury models [19–27].

Since pulmonary microvascular EC CN PDEs have not been characterized previously, the studies reported here were directed toward defining the functional isoforms of pulmonary microvascular EC PDE families in comparison to other ECs. PDE4 isoforms were the dominant enzymes in these ECs. The results of a portion of these studies have been published in abstract form [28].

2. Materials and methods

2.1. Materials

[2,8-^{3}H]cAMP (sp. act. 36.5 Ci/mmol) and [8-^{3}H]cGMP (sp. act. 18 Ci/mmol) (Morovitz), Dowex-1 X8 (200–400) resin (Aldrich Chemical Co.), and DEAE-trisacryl M (IBF) were purchased and prepared as described previously [29]. Benzamidine tosyl-lysyl-chloroketone (TLCK), aprotinin, pepstatin A, and porcine gelatin were from the Sigma Chemical Co., and leupeptin was from Peninsula Laboratories. CN PDE inhibitors were purchased from BioMol Inc. or synthesized by others as described previously [30]. Drugs were dissolved in ultrapure DMSO (Aldrich), and the solvent was diluted to <0.25% in enzyme or culture assays. Rat collagen IV and Matrigel were purchased from Collaborative Biomedical Products, and DiI-conjugated acetylated low-density lipoprotein (DiI-ac-LDL) was obtained from Biomedical Technologies. PDE4A and PDE4B carboxy-terminal peptide (CTP-PDE4A and CTP-PDE4B) subfamily-selective rabbit antiserum or PDE4D (M3S1) subfamily-selective mouse monoclonal antibodies were used. M3S1 and AC55 (PDE4A-selective) antisera were provided by M. Conti, Department of OB/Gyn, Stanford University Medical Center. CTP-PDE4A and CTP-PDE4B were prepared based on the studies of Houslay and colleagues [31], and Bolger *et al.* [32] using the carboxy-terminal peptide antigens EAQREHQAAKRAC and CDIDATEDKSPVDT, respectively, coupled to KLH (Bethyl Laboratories). Antisera to peptides were affinity-purified with peptide antigen covalently linked to Sepharose 4B using citrate/phosphate, pH 2.2, buffer elution. Sheep antibodies to the cGMP binding regions of PDE2 and 5 (CTLAFQKEQKLKCECQA; CAQLYETSLLENKRNQV) (cGB-PDE2; cGB-PDE5) [33] were also prepared (Bethyl Laboratories), and were affinity-purified as already described. Peroxidase-coupled goat anti-rabbit IgG antibodies were purchased from Zymed and used as secondary antibodies for Western blot visualization. Preimmune sera were purified as IgG fractions using HiTrap NHS-activated Sepharose anti-IgG columns. Reverse transcription-polymerase chain reaction (RT-PCR) kits were obtained from Stratagene, RNA-STAT from Tel-test "B" Inc., and an Oligo-dT kit from 5′ to 3′ Inc.

2.2. EC preparation, culture, and characterization

Primary isolates of RPMVEC were obtained from perfused rat lung and cultured in our laboratory [34]. An established RPMVEC cell line was provided by U.S. Ryan (T Cell Diagnostics). RPMVEC were used from passage 4 through passage 31, and the established line was received at passage 55 and used to 120. The cells were grown in Dulbecco's minimal essential medium (DMEM) containing 10% fetal bovine serum (FBS) (Intergen), 0.1% penicillin/streptomycin, 0.05% amphotericin B, and 0.1% gentamicin (Gibco and Sigma). Neither microvascular EC culture showed a propensity to expire after 15–25 passages, as is often characteristic of ECs from conduit vessels [35]. Each showed a characteristic cobblestone morphology at confluence, indirect immunofluorescence with factor VIII antigen antibody binding, uptake of DiI-ac-LDL, and induction of capillary-like structures on Matrigel [34,35]. Cells from both sources retained atriopeptin II receptors as shown by enhanced cGMP accumulation with $EC_{50} = 4$ nM [35] and β-adrenergic receptors (*vida infra*).

2.3. Intact EC cAMP accumulation

cAMP accumulation in intact RPMVEC was studied using prelabeling techniques as described previously [30,36]. RPMVEC were harvested by scraping and allowing major clumps of undispersed cells to settle. The remaining suspended cells were seeded in 6-well plates at approximately 200,000 per well and grown for 3 days to preconfluence or near 10^6 cells per well. DMEM with 10% FBS was replaced with 2 mL medium containing 2 Ci [^{3}H]-adenine/mL and incubated for 1 hr in a CO_2 incubator to label cellular ATP. Unincorporated tritium in medium was aspirated and replaced with DMEM containing test drug or vehicle in the absence of serum. Reactions were terminated by rapidly aspirating the medium and applying 1 mL of 5% trichloroacetic acid (TCA) containing [^{14}C]cAMP tracer. [^{3}H]cAMP was purified by Dowex-50/neutral alumina double-column chromatography. Recoveries from each column and cAMP conversion from ATP were calculated from double-label scintillation counting as described previously [30].

2.4. CN PDE assay

CN PDE activities were determined using the two-step isotope method [29] as described previously with 0.25 μM [^{3}H]cAMP (100,000 cpm) or 0.5 μM [^{3}H]cGMP

(100,000 cpm) substrate. For analysis of calcium and calmodulin sensitivity, the cGMP substrate was used at 25 μM, and the assay mixture contained 50 ng calmodulin with or without 0.5 mM EGTA and 1 mM calcium. The apparent K_m values were determined using cAMP from 0.06 to 10 μM with 300,000 cpm. cGMP activation of cAMP hydrolysis was determined using 5 μM substrate and 2 μM cGMP. Inhibitors (0.01–50 μM) were studied with 0.125 μM [^{3}H]cAMP substrate. Kinetic parameters and inhibition constants were calculated using the Prism 2.1 program (GraphPad). Protein was measured by the method of Bradford [37] with BSA as standard.

2.5. Western blot analysis

The 100,000 *g* supernatants of passage 4–10 RPMVEC were used for immunoblot analyses. Cells from confluent T-75 flasks were scraped off of the culture surface, pelleted at low speed (1500 rpm in an IEC Pr6000 centrifuge at ambient temperature for 10 min), and homogenized in 0.25 mL of homogenizing buffer [homogenized in 5 vol.% of 20 mM Tris–acetate (pH 7.4), 5 mM $MgCl_2$, 10 μM TLCK, 2000 units aprotinin/mL, 2 μM leupeptin, 2 μM pepstatin A, 10 μM benzamidine (TMPI)] with a Duall-type glass homogenizer using 20 strokes of a Teflon pestle by hand as described previously [37]. A 105,000 *g* supernatant was prepared and precipitated using chloroform/methanol. Fifty micrograms of protein was applied to each lane and separated by 7.5% SDS-PAGE with a Novex mini-gel apparatus and electrophoretically transferred to nitrocellulose paper (0.2 μm; Schleicher & Schuell Inc.) as described previously [38]. Ponceau S staining was used to verify transfer and define molecular weight markers (K_D = 205, 116, 97.4, 67, 55, 35, 31). PDE4 immunoreactivities were detected after protein blocking (Boehringer) with PDE4A-selective CTP-PDE4A and PDE4B-selective CTP-PDE4B polyclonal antisera. Detection was with horseradish peroxidase (HRP)-linked goat anti-rabbit IgG or rabbit anti-mouse IgG using BM Teton substrate (Boehringer–Mannheim) and 0.02% hydrogen peroxide. PDE4D-selective M3S1 monoclonal antibody and AC55 PDE4A-selective antisera were used to verify the affinity-purified CTP immunoreactivities. In addition, PDE1, 2, and 5 selective antisera were used in conjunction with mRNA transcript analyses.

2.6. RT-PCR

Total RNA from preconfluent RPMVEC from five 100 mm^2 plates [5] was isolated using 1 mL RNA-STAT per plate on ice. Passage 5 cell lysates were frozen, thawed, and processed for RNA using chloroform, isopropanol, and ethanol washes according to the instructions of the manufacturer. Each RNA preparation had an optical density (260/280 ratio) >1.8 and a total yield of approximately 500 μg. Poly(A)$^+$-RNA was purified using Oligo-dT columns from 5′ to 3′ Inc. according to instructions with the kit. Total RNA (30 μg) or mRNA (0.8 μg) was reverse transcribed in 50 μL RT buffer containing 300 ng random primers, 40 units RNAse inhibitors, 1 mM dNTP (Perkin-Elmer), and 50 units MMLV-RT for 60 min (37°). PCR was performed with 3–8 μL of RT product cDNA in 50 μL containing 1 unit Taq polymerase (Perkin-Elmer), 20 μM dNTP, 1.5 mM $MgCl_2$, buffer, and 300 ng forward and reverse primers. The amplification protocol in a Perkin-Elmer 9600 thermocycler incorporated 35 cycles of 5 min at 94° (denaturation), 30 s at 50° (annealing), 1 min at 72° (extension). RT-PCR products were separated by 0.8 or 1.2% agarose (Gibco-BRL) or 7.5% acrylamide gel electrophoresis. Primer sequences were chosen from alignments of GenBank rat PDE sequences to differentiate gene families. Primer–dimer and false priming were minimized using the program Oligo 5 and GenBank searches. Forward and reverse primers to resolve PDE families, expected product sizes (bp), and annealing temperatures were: PDE1, 5′-ATCCACGACTATGAGCACACT-3′ and 5′-TCCTTGTCACCCTGGCGGAGAAT-3′ (399, 56°); PDE2, 5′-CCCAAAGTGGAGACTGTCTACACCTAC-3′ and 5′-CTGGCCACAGTGCACCAAGATGA-3′ (254, 60°); PDE3, 5′-TCACCTCTCCAAGGGACTCCT-3′ and 5′-CAGCATGTAAAACATCAGTGGC-3′ (700, 60°); PDE5, 5′-GTGAAAGATATTTCTAGTCACTTG-3′ and 5′-ATACATGGTAATTGATTCTGTTTGC-3′ (768, 52°); and PDE7, 5′-GCTCTCTTCGGCTGCCCCAAT-3′ and 5′-ACGAAGTTTCATCATATCTAA-3′ (487, 50°). Primers for PDE4 isoforms were chosen to resolve subfamily RNA transcripts. These were: PDE4A (all forms) 5′-GCTTGAACACCAACGTCCCACGGT-3′ and 5′-GCTGAGGTTCTGGAAGATGTCGCAG-3′ (539, 60°); PDE4B (all forms) 5′-ATGACCCAGATAAGTGGAGTGAAG-3′ and 5′-TCAGGCTGAACCAGGTCTGCCCAG-3′ (998, 68°); PDE4C (both forms) 5′-ATGGCCCAGATCACTGGGCTGCGG-3′ with the same reverse primer as PDE4A (582, 60°); and PDE4D (all forms) 5′-ATGGCCTCCAACAAGTTCAAGAGG-3′ and 5′-GCTGGCTTTCCTCTTCTGCTACAGCC-3′ (1480, 60°). Each positive band from 0.8% agarose gels was reamplified with the same primers, cloned into pCR2.1 vector, and sequenced at the USA Biopolymer Core Laboratory using an ABI 377 sequencer.

2.7. CN PDE fractionation with DEAE-trisacryl M chromatography

Preconfluent early or late passage cells were scraped from 150 mm tissue culture dishes after two washes with cold PBS for PDE isoform fractionation. Trisacryl M anion-exchange chromatography was used with either discontinuous or continuous salt gradients to separate PDE activities. Passages 4, 10, 31, 59, and 125 RPMVEC from 5 to 10 dishes (approximately 7.5×10^7 cells) were pelleted at low speed (1500 rpm in an IEC Pr6000 centrifuge at ambient temperature for 10 min) and homogenized in 5 vol.% of TMPI with a Duall-type glass homogenizer using 20 strokes

of a Teflon pestle by hand as described previously [37]. A 105,000 *g* supernatant was prepared and applied to a DEAE-trisacryl M column with a 4 mL bed volume equilibrated with homogenization buffer. The high speed supernatant contained approximately 79% of the cAMP PDE activity from the homogenate measured at 0.25 μM cAMP substrate. The column was washed with 20 mL of homogenization buffer, and PDE activities were eluted with successive linear gradients of 15 mL of 0–150 mM and 20 mL of 150–500 mM NaCl or a linear 40 mL gradient from 0 to 500 mM in homogenization buffer at a flow rate of 0.5 mL/min. The 100,000 *g* particulate fraction after resuspension in homogenization buffer contained less than 5% of the total homogenate activity. cGMP-stimulated, cGMP-inhibited, or calmodulin/calcium-stimulated cAMP PDE activities were not detected in the particulate or supernatant fractions using standard assay conditions.

3. Results

3.1. Time courses of rolipram-, forskolin-, and isoproterenol-induced cAMP accumulation

Extended time courses of rolipram-induced cAMP accumulation in RPMVEC were determined using intact cell prelabeling in the presence and absence of isoproterenol and forskolin (Fig. 1). Rolipram at 10 μM showed a peak of cAMP accumulation at approximately 30 min and was more effective than either forskolin or isoproterenol alone (top panels). The increases in either isoproterenol- or forskolin-induced cAMP accumulations with rolipram were significantly greater as shown in the lower panels. Different scales on the *y*-axis were required due to their large combined effects. Isoproterenol and forskolin were not very effective inducers of cAMP accumulation in these cells in the absence of rolipram even at concentrations 10 times their respective EC_{50} values, suggesting a major role of PDE4 in regulating cAMP metabolism in RPMVEC.

In the presence of 10 μM rolipram, the EC_{50} for forskolin-induced cAMP accumulation was 1.1 μM with a 15 min treatment (Fig. 2). Similarly, in the presence of 10 μM rolipram, the EC_{50} for isoproterenol-induced cAMP accumulation was near 1 μM (15 min accumulation; data not shown). With a protocol of 1 hr prelabeling and a 5 min preincubation with rolipram, cAMP accumulation induced by adenosine-5′-(*N*-ethylcarboxamide) (NECA), a non-selective adenosine receptor agonist, was also enhanced (Fig. 3). In addition, rolipram was effective using NECA and an A_1-adenosine receptor blocker, 8-phenyltheophylline, or using 2-*p*-(2-carboxyethyl)phenethylamino-5′-*N*-ethylcarboxamido adenosine (CGS 21680), a selective

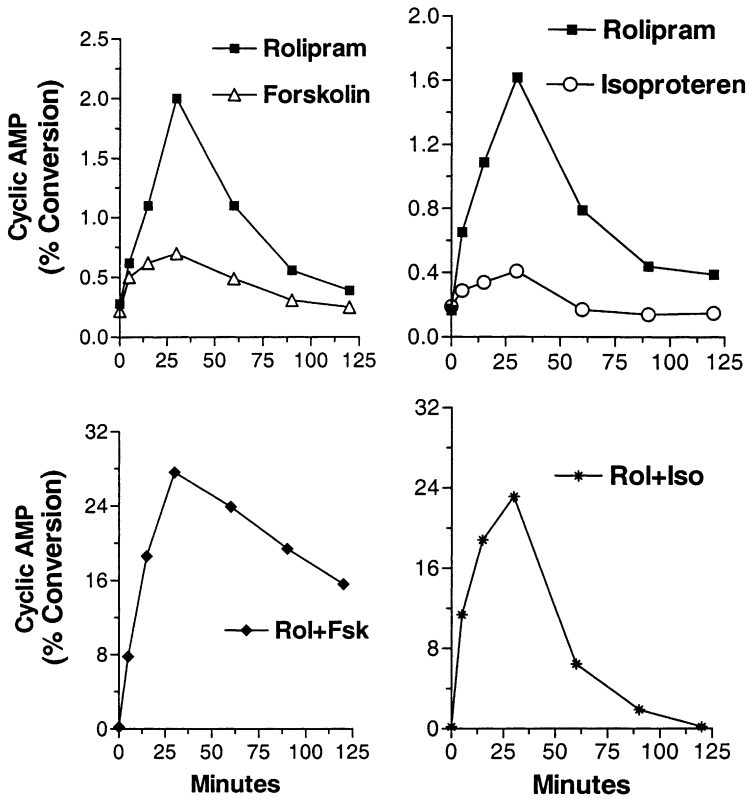

Fig. 1. Time course of rolipram potentiation of forskolin- and isoproterenol-induced cAMP accumulation in RPMVEC. RPMVEC cAMP accumulation in the presence and absence of forskolin, isoproterenol, or rolipram (10 μM) was studied using prelabeling techniques as described in Section 2. RPMVEC were seeded and grown in 6-well plates to near 10^6 cells per well, and cellular ATP was prelabeled for 1 hr. Cells were washed and treated with drugs in DMEM in the absence of serum. Reactions were terminated with 5% TCA containing [^{14}C]cAMP tracer. [^{3}H]cAMP was purified, and percent conversion was calculated as described in Section 2. Data are the means of triplicates from one experiment repeated three times. Individual values varied by less than 10%.

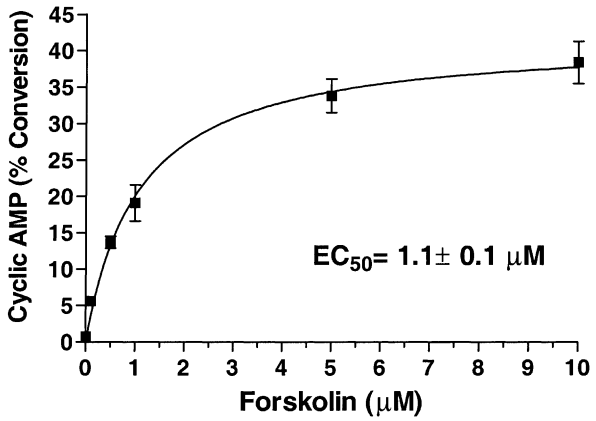

Fig. 2. RPMVEC forskolin concentration–response in the presence of rolipram. cAMP accumulation in intact RPMVEC induced by various concentrations of forskolin (0–10 μM) in the presence of rolipram (10 μM) was studied using prelabeling techniques as described in Section 2. RPMVEC cellular ATP was prelabeled for 1 hr, and washed cells were treated for 10 min in DMEM in the absence of serum. [^{3}H]cAMP was purified, and percent conversion was calculated as described in Section 2. Data shown are means ± SEM of triplicates from one experiment repeated three times.

A_2-adenosine receptor agonist (Fig. 3), indicating that PDE4 is coupled to adenosine (A_2) receptors as well as β-adrenergic receptors.

3.2. Inhibitor sensitivity of RPMVEC cAMP PDE

The effects of selected PDE inhibitors were studied using trisacryl M fractionated enzyme preparations. The concentrations of the drugs inhibiting cAMP hydrolysis by 50% (IC_{50}) using 0.25 μM substrate and 5 mM magnesium were as expected for PDE4 isoforms. The order of potency for the *in vitro* inhibition of the peak activity was rolipram, trequinsin, 1-ethyl-4-(ethylthio)-1*H*-pyrazolol[3,4-*b*]-pyridine-5-carboxylic acid, ethyl ester (SQ65442), and IBIAX ($IC_{50} = 0.2-0.4\,\mu M$) > RO 20-1724 and papaverine ($IC_{50} = 0.9\,\mu M$) > dipyridamole, CGS-9343B, MIX, and CK-0383 ($IC_{50} = 2-10\,\mu M$)⋙CGS-9343B, indolidan, theophylline, 7-propargyl- and 7-benzyl-MIX, 8-methoxymethyl- and 8-*t*-butyl-MIX, zaprinast, CK-3197, CK-2130 ($IC_{50} > 50\,\mu M$).

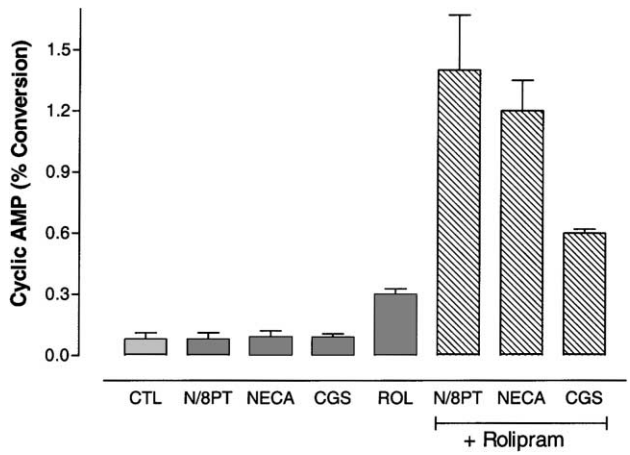

Fig. 3. Intact cell RPMVEC rolipram response in the presence of adenosine receptor agonists. cAMP accumulation was determined as described in Section 2 and Fig. 1. Rolipram was added for 5 min before the agonists, with 10 min of incubation. Data shown are the means ± SEM of triplicate wells. N/8PT = NECA plus 8-phenyltheophylline, CGS = CGS 21680.

3.3. Inhibitor sensitivity of isoproterenol- and forskolin-induced cAMP accumulation in intact EC

Several of the PDE inhibitors used *in vitro* were tested further for their effects on potentiation of intact cell isoproterenol-induced cAMP accumulation. RPMVEC were prelabeled with [^{3}H]-adenine for 1 hr, and [^{3}H]cAMP μM isoproterenol for 10 min in the presence of different PDE inhibitors given 5 min before isoproterenol (Fig. 5). Indolidan, zaprinast, dipyridamole, and 8-*t*-butyl-MIX, drugs that were not effective inhibitors *in vitro*, also had no effect on cAMP accumulation alone (data not shown) or when combined with isoproterenol (Fig. 5). In contrast, the drugs with submicromolar IC_{50} values for inhibition of PDE4 activity on enzyme functions (IBIAX, SQ65442, trequinsin, and rolipram) all demonstrated enhanced cAMP accumulation in response to isoproterenol (Fig. 5).

3.4. Comparative effects of PDE4 inhibitors on isoproterenol-induced cAMP in intact ECs

The effects of PDE4 inhibitors on prelabeled (1 hr) intact RPMVEC exposed to 10 μM isoproterenol were compared further with respect to concentration (Fig. 4) and time

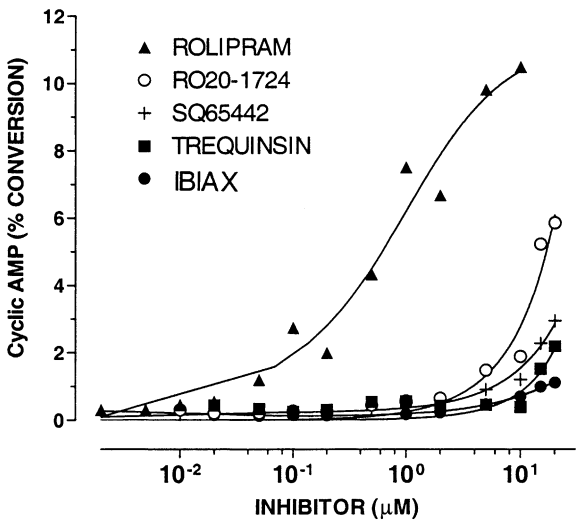

Fig. 4. Concentration–responses for high-affinity PDE inhibitor potentiation of isoproterenol-induced cAMP accumulation in RPMVEC. cAMP accumulation in intact RPMVEC was induced by isoproterenol (10 μM; 10 min) and studied using prelabeling techniques as described in Fig. 1. Inhibitor preincubation was for 10 min. Data shown are from one experiment repeated, in part, two times. Rolipram, SQ65442, trequinsin (HL-725), and IBIAX showed IC_{50} values *in vitro* from 0.2 to 0.4 μM, and for RO 20-1724 $IC_{50} = 0.9\,\mu M$.

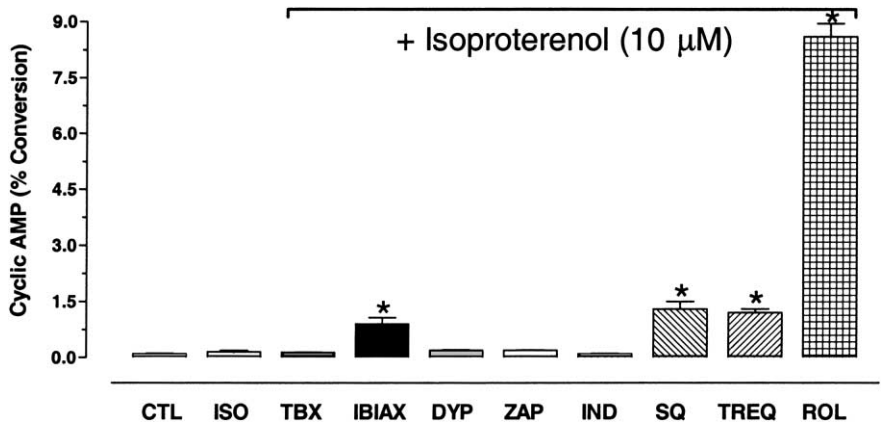

Fig. 5. cAMP PDE inhibitor potentiation of isoproterenol-induced cAMP accumulation in RPMVEC. cAMP accumulation in intact RPMVEC induced by isoproterenol (10 μM) was studied using prelabeling techniques as described in Section 2. RPMVEC, prelabeled and processed as in Fig. 1, were washed and treated with PDE inhibitors for 5 min, and isoproterenol was added for an additional 10 min in DMEM in the absence of serum. Data shown are means ± SEM of triplicates from one experiment repeated three times. Isoproterenol (ISO), *t*-butylxanthine (TBX), rolipram (ROL), SQ65442 (SQ), dipyridamole (DYP), zaprinast (ZAP), indolidan (IND), trequinsin (TREQ), and isobutyl-isoamyl-methylxanthine (IBIAX) were used at 20 μM, (∗) significantly different from control or isoproterenol, $P < 0.05$.

responses (Fig. 6). Despite similar inhibition constants *in vitro*, rolipram was considerably more effective than the other PDE4 inhibitors when studied in the intact cell. For example, rolipram was effective at much lower concentrations than were 4-(3-butoxy-4-methoxy benzyl)-2-imidazolidinone (RO 20-1724), trequinsin (HL 725), SQ65442, or IBIAX and showed a much higher intrinsic activity (i.e. greater maximum response) in enhancing cAMP accumulation in response to 10 μM isoproterenol (Fig. 4).

To determine if the length of time that the PDE inhibitor was present might have influenced the apparent intrinsic activity of the isoproterenol/inhibitor combination, drugs were added at various times during the course of a 15 min isoproterenol incubation. Drugs other than rolipram showed a peak in their maximum responses at 5–10 min, whereas the effects of rolipram continued to increase throughout the incubation period (Fig. 6).

3.5. Reversal of rolipram- and isoproterenol-induced cAMP accumulation in intact ECs

RPMVEC prelabeled with [^{3}H]-adenine were incubated with 10 μM rolipram and 10 μM isoproterenol for 15 min. The medium containing the drugs was aspirated rapidly and replaced with drug-free DMEM. The decay of accumulated [^{3}H]cAMP in the cells was determined. When the results were plotted on a semi-log scale, a linear first-order decay process with a $T_{1/2}$ of approximately 4 min was indicated (Fig. 7).

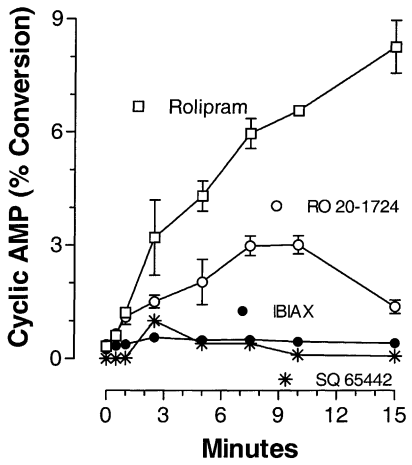

Fig. 6. Time courses of high-affinity PDE inhibitor potentiation of isoproterenol-induced cAMP accumulation in RPMVEC. cAMP accumulation in RPMVEC in the presence of isoproterenol with RO 20-1724, IBIAX, SQ65442, or rolipram (10 μM) was studied using prelabeling techniques as already described. Data shown are the means ± SEM of triplicates from separate experiments for each inhibitor. Where error bars are not shown, these values are included within the data symbols.

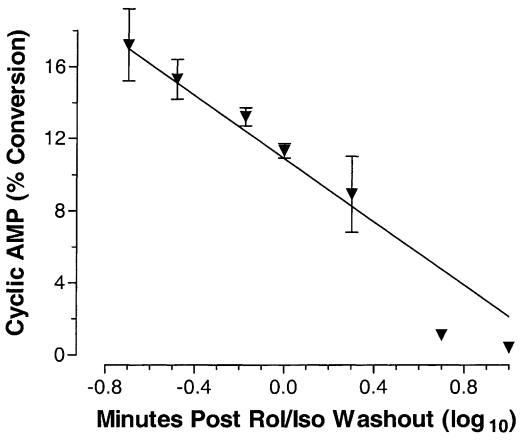

Fig. 7. Kinetics of the reversal of rolipram/isoproterenol-induced cAMP accumulation in RPMVEC. cAMP accumulation was stimulated with 10 μM rolipram and isoproterenol for 15 min, and the decay of accumulated [^{3}H]cAMP in the cells was determined with drug-free DMEM. With first-order decay, the $T_{1/2}$ was calculated from the slope of the line as determined by linear regression. Values shown are means ± SEM of triplicate culture wells.

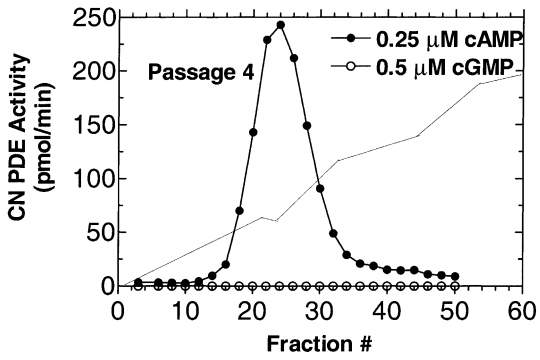

Fig. 8. Anion-exchange chromatography of cAMP PDE in RPMVEC. Microvascular EC supernatants were prepared from passage 4 cells (approximately 7.5×10^7) and separated on trisacryl M DEAE-cellulose columns (4 mL) as described in Section 2. A single peak of cAMP PDE activity eluted at approximately 0.16 M NaCl in passage 4. PDE activity was eluted with a linear 40 mL gradient from 0 to 500 mM in homogenization buffer at a flow rate of 0.5 mL/min. cAMP and cGMP substrate concentrations were 0.25 and 0.5 μM, respectively. cGMP hydrolysis was not detected in the supernatant or column fractions. This profile is representative of three different preparations of supernatant extracts prepared as described in Section 2.

3.6. Anion-exchange chromatography of RPMVEC cAMP PDE

Microvascular endothelial cell supernatants fractionated on trisacryl M DEAE-cellulose columns showed a single peak of cAMP PDE activity eluting at approximately 0.16 M NaCl in passage 4 ECs (Fig. 8) and passage 31 and 59 ECs (data not shown). This ionic strength was shown previously to elute PDE1, 2, and 5 cGMP PDE activities from other EC types and from different tissues [38–41]. Minimal cGMP hydrolysis was detectable in supernatant or column fractions of these cells.

The kinetic behavior of the trisacryl M peak activity from passage 4 cells with cAMP substrate showed a linear Hofstee–Eadie plot of the data from which an apparent $K_m = 0.8$ μM for cAMP was calculated.

An unusual feature of RPMVEC, unlike EC cultures isolated from other anatomical locations [38], is the stability of these cells in culture [35]. RPMVEC isolated in our laboratory have been expanded from passage 4 cultures through subsequent passages (40 and greater) with no changes in morphology or growth rate. The established RPMVEC line provided by Ryan (see Section 2) also maintained culture stability. Trisacryl M fractionation of passage 12 supernatant showed single peaks of cAMP PDE activity eluting at an ionic strength similar to passage 4 cells and with no cGMP hydrolysis (data not shown). Thus, both the primary and the established cell line for early and late passage RPMVEC expressed PDE4 isoforms with minimal or no measurable cGMP PDE activities.

3.7. Western blots of RPMVEC supernatant PDEs

High speed supernatants of RPMVEC cell pellets from confluent cells were prepared with a small volume hand-held homogenizer, precipitated, and concentrated. The

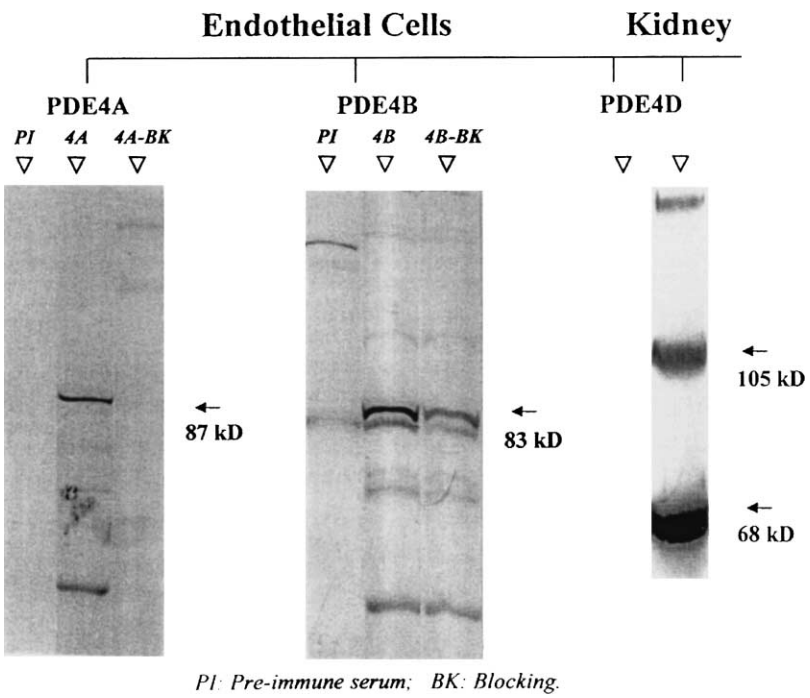

Fig. 9. Western blot analysis of CN PDE isoform expression in RPMVEC. Supernatants (100,000 *g*) of passage 4–10 RPMVEC or rat kidney were prepared and precipitated as indicated in Section 2. The fractions (50 μg protein) were separated by 7.5% SDS-PAGE and electrophoretically transferred to 0.2 μm nitrocellulose. The detection of PDE4 on immunoblots was performed by using affinity-purified PDE4 subfamily-selective antiserum as described in Section 2; the immunoreactivities of 4A (left), 4B (middle), and 4D (right) are shown. The immunoblots were also exposed to either purified pre-immune serum (PI) or antibodies to blocking peptides (BK) for PDE4A or PDE4B. Detection was with HRP-linked secondary antibodies with BM Teton substrate and 0.02% hydrogen peroxide.

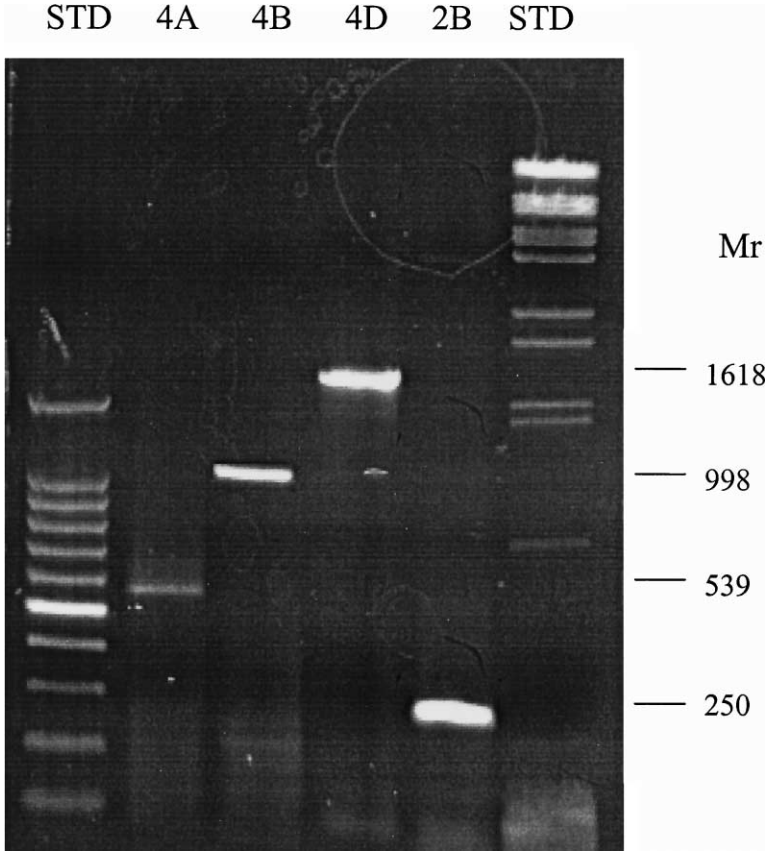

Fig. 10. PDE4 RNA analysis by RT-PCR in RPMVEC. Total RNA or poly(A)$^+$-RNA was isolated, purified, and reverse-transcribed as described in Section 2. RT product cDNA was amplified in a Perkin-Elmer 9600 thermocycler using 35 cycles of 5 min at 94° (denaturation), 30 s at 50° (annealing), 1 min at 72° (extension). The RT-PCR products, identified by agarose electrophoresis as described in Section 2, are shown in lanes 2–5 with their sizes relative to standards in lanes 1 and 6. Forward and reverse primers designed from aligned rat sequences were used to resolve PDE1, 2, 3, 5, and 7 gene families and PDE4 (all forms) along with subfamilies PDE4A, B, C, and D (all forms). Each positive band from 0.8% agarose gels was reamplified, cloned into pCR2.1 vector, and sequenced at the USA Biopolymer Center using an ABI 377 sequencer.

representative Western blots of PDE immunoreactive bands separated by 7.5% SDS-PAGE are shown in Fig. 9. The left lanes show the immunoreactivity of PDE4A polyclonal antisera, preimmune serum, and blocking peptides. The major immunoreactive protein was detected at 87 kDa with minor bands occasionally seen at 40 kDa, probably representing partially proteolyzed enzyme. The peptide antibody K116 that recognizes PDE4 family isozymes, and the antisera AC55 which is selective for PDE4A forms [42], also showed reactivity at 87 kDa (data not shown). The PDE4B-selective peptide antisera showed a dominant 83 kDa 4B isoform, which was not detected with preimmune serum, and was blocked by peptide antigen (middle lanes). Monoclonal antibody M3S1, selective for subfamily PDE4D, showed no reactivity to the RPMVEC supernatant but did react with a rat kidney supernatant positive control (right lanes). Antisera to PDE1, 2, and 5 isoforms were negative (data not shown).

3.8. RT-PCR of RPMVEC

RT-PCR was used to identify subfamilies of PDE4 in RPMVEC. Using total RNA or mRNA, primers selective for 4A, B, and D subfamilies of PDE4 were positive (Fig. 10, lanes 2–4, respectively). These results were verified by subcloning and sequence analyses. Forward and reverse primers selective for PDE4C transcripts did not produce DNA using up to 40 cycles of PCR and 5 μg mRNA. RT-PCRs using primers selective for other PDE families including 1, 3, 5, and 7 were negative. However, transcripts for PDE2B were found (lane 5, Fig. 10) and verified by sequence analysis. Thus, unlike PDE4A and 4B activities, both PDE2 and PDE4D mRNAse are transcribed in RPMVEC, but are not translated to active enzymes.

4. Discussion

RPMVEC showed an active and functional CN PDE4 isoform exclusive of the isozymes of other major PDEs in these cells. The PDE4 isoforms are of the 4A and B subfamilies, as shown by RT-PCR and Western blot analysis with specific antisera. Although PDE4C mRNA was not detectable, PDE4D and PDE2 mRNA transcripts were identified by RT-PCR analysis. However, no immunoreactive protein was found for PDE4D or PDE2 activity using

isoform-specific antibodies. RPMVEC PDE4 showed a characteristic high affinity and specificity for cAMP substrate with Michaelis–Menten kinetic behavior. This isoform combination lacked negative cooperative behavior or multiple affinity kinetics that is characteristic of high-affinity cAMP hydrolysis in some tissues and cells [8,29].

Inhibitor studies of RPMVEC PDE4 activity revealed a group of drugs: (rolipram, RO 20-1724, isoamyl-isobutyl xanthine, trequinsin, and SQ65442) with submicromolar inhibition constants. Thus, PDE4 isoforms appear to be the primary regulator of cAMP hydrolysis in this cell type as seen for these agents in other sources of ECs [38,40,41].

The effects of the PDE4 inhibitors were studied further using intact cell [^{3}H]-adenine prelabeling, an experimental method to analyze the effects of PDE inhibitors in the intact cell [30,36]. Furthermore, since RPMVEC did not express other PDE isoforms, these cells offered a unique way to compare the cellular effects of these inhibitors with their *in vitro* inhibition constants on a specific PDE isoform. These comparisons showed that: (i) the inhibitors needed to be of high affinity *in vitro* to achieve maximal cAMP accumulation in the presence or absence of isoproterenol- or forskolin-induced cAMP accumulation. For example, the inhibitors with low affinity *in vitro* did not potentiate intact cell cAMP accumulation effectively; (ii) rolipram produced greater cAMP accumulation in the intact cell than did either forskolin, isoproterenol, or adenosine derivatives in the absence of PDE inhibitors; and (iii) although PDE4-selective drugs had comparable submicromolar IC_{50} values *in vitro*, they did not show the same apparent EC_{50} values for cAMP accumulation in the presence of adenylate cyclase agonists in the intact cell assays.

Rolipram, when used alone, caused a much greater increase in cAMP accumulation than did other PDE4 inhibitors despite similar potencies *in vitro* to inhibit cAMP hydrolysis. Several possibilities could account for these differences: (i) subtypes of PDE4 isoforms could be differentially affected by rolipram; (ii) the marked increase in cAMP accumulation induced by rolipram may result from very high basal adenylate cyclase activity in these cells; (iii) elevations of cAMP in response to rolipram action may alter PDE profile in these cells; and (iv) the actions of rolipram are only partially attributed to its ability to inhibit PDE4 directly. In this regard, high-affinity binding of rolipram and related analogues does not correlate with their *in vitro* potency as PDE4 inhibitors. Although, we have observed changes in PDE profiles following long-term exposure of microvascular ECs to rolipram in culture (manuscript in preparation), no difference in inhibitory potency of the drug on fractionated enzyme preparations of these activities was noted. The data described in Fig. 7 on the rate of decay ($T_{1/2}$ of 4 min) of cAMP after removal of rolipram indicates a very high turnover rate for cAMP in these cells governed largely by PDE. The data in Fig. 6 in which PDE inhibitors were added at various times after treatment with isoproterenol for 15 min also suggest the significant involvement of PDE in cAMP turnover. The accumulation of cAMP reached a plateau within 5–10 min for PDE4 inhibitors other than rolipram. In contrast, cAMP continued to accumulate in the cells at the later time periods indicating differences in the actions of rolipram as opposed to the other agent, e.g. different effects on the extrusion of cAMP for the cells might contribute to these differences. The intrinsic activities of these PDE4-selective inhibitors varied in the intact cell. In settings of drug discovery, comparisons of intact cell effects of PDE4 inhibitors with *in vitro* data are important since the intrinsic activities of these drugs are dependent upon other factors or processes in addition to PDE4 high-affinity inhibition. Rolipram has also been shown to be more effective than other PDE4 inhibitors on forskolin-induced cAMP accumulation in porcine aortic EC [8].

Since rolipram is an effective inhibitor of PDE4 subfamily A–D isoforms, it seems unlikely that isoform expression accounts entirely for the enhanced rolipram sensitivity observed in microvascular cells. One property of rolipram that is inconsistent with its inhibition constants is its high-affinity binding site on the enzyme [14]. This discrepancy has led to the concept of higher- and lower-affinity conformations of the enzyme in equilibrium [43,44]. High-affinity binding of rolipram has been studied extensively, and analogues expressing a binding affinity greater than their catalytic affinity are more likely to produce the emetic action of rolipram and many other PDE4 inhibitors [44,45]. Therefore, in ECs, high-affinity inhibitor binding could contribute to the higher intrinsic activity seen in the intact cell. Therefore, we tested the possibility that longer incubations with the less effective inhibitors would allow greater cAMP accumulation in response to isoproterenol. Extended time courses did not improve the maximal effect (i.e. the intrinsic activity) of these inhibitors. Alternatively, if a high-affinity binding site was involved in the greater accumulation of cAMP in RPMVEC, a relatively slow dissociation of the drug would be expected from such a site. The reversal of rolipram-induced cAMP accumulation with isoproterenol was very rapid in the intact cell with a $T_{1/2}$ of approximately 4 min, a first-order rate constant inconsistent with high-affinity binding of the drug in the intact cell. Thus, the high-affinity rolipram binding is not likely to be the primary reason for the greater intrinsic activity of rolipram as compared with other PDE4 inhibitors.

This study of microvascular EC PDE used probes of PDE gene families, subfamilies, and spliced variants developed in several laboratories [43,46,47]. However, only a few studies have correlated mRNA analysis, PDE protein expression, and intact cell activity [42,45,47]. The RPMVEC PDE4A spliced variant found was one of the "long" forms, PDE4A6 (RPDE39), identified at 87 kDa by PDE4A-selective antisera. The PDE4A6 isoform was also confirmed by RT-PCR (Kelly *et al.*[4]). We also found that

[4] Unpublished data.

the long form of the PDE4B gene, 4B3, at 83 kDa was present in RPMVEC and appears similar in rat cortex and cerebellum [42]. Confocal microscopy of fixed and permeabilized RPMVEC showed immunoreactivity to PDE4A in cytosolic and perinuclear locales; plasma membrane immunoreactivity was not observed (data not shown) [31,44].

Isoforms of PDE gene families 1–7, with the exception of PDE6, have been noted in varying amounts in ECs depending upon the source of the cells and culture conditions. In early passage aortic vessel ECs, PDE2 and PDE4 isoforms predominate along with small amounts of PDE5 (Lugnier and Schini [39], Souness *et al*. [40], and Kishi *et al*. [41]). However, Ashikaga *et al*. [38] found major changes in PDE isoforms in bovine aortic EC cultures as a function of culture conditions. For example, PDE2 and PDE5 activities were lost, and PDE1 and small amounts of PDE3 were detected with cell passage as was seen in other types of EC by Seid *et al*. [48], and Suttorp *et al*. [49]. The isoform changes were also accompanied by a dramatic increase in PDE4 in the higher passage cultures [38]. High-speed supernatants from both early and late passage primary microvascular EC cultures showed stable PDE4 expression, a finding in contrast with EC cultures from large vessels. A significant finding in RPMVEC was the lack of appreciable cGMP hydrolysis, a result consistent with our previous study using intact cell cGMP turn-over analysis [36]. The detection of PDE2 mRNA without the detection of active enzyme or immunoreactive protein indicates another level of complexity of PDE isoform expression. However, the stability of mRNA and the possible regulation by cAMP in these cells have not been investigated. Further, studies will be required to determine if microvascular or conduit ECs from tissues other than lung are similar or distinguishable on the basis of PDE isoform expression.

In summary, PDE4 is the dominant enzyme in RPMVEC and regulates cAMP metabolism in these cells. High-affinity inhibitors of PDE4 activity are effective inducers of cAMP in RPMVEC, and these drugs interact synergistically with agonists of cAMP synthesis in these cells. The intrinsic activities of PDE4 inhibitors in the intact cell do not correlate with their IC_{50} values *in vitro* to inhibit isoform-specific PDE4 CN PDE. These studies provide a biochemical and molecular basis to conclude that the mechanism of rolipram reversal of rat lung ischemia-reperfusion-induced permeability injury involves selective PDE4 inhibition in microvascular ECs by a relatively potent PDE4 inhibitor.

Acknowledgments

The authors are indebted to Raymond Hester, Director of the University of South Alabama College of Medicine Research Cytometry Laboratory, for his aid with confocal microscopy. The excellent technical assistance of Druhan Lowry, Kelly Morgavio, Tashandra Underwood, and Raquel Dien is recognized. This research was supported by USPHS Grant HL-46494.

References

[1] Barnard JW, Seibert AF, Prasad VR, Smart DA, Strada SJ, Taylor AE, Thompson WJ. Reversal of pulmonary capillary ischemia-reperfusion injury by rolipram, a cAMP phosphodiesterase inhibitor. J Appl Physiol 1994;77:774–81.

[2] Martin W, White DG, Henderson AH. Endothelin-derived relaxing factor and atriopeptin II elevate cyclic GMP levels in pig aortic endothelial cells. Br J Pharmacol 1988;93:229–39.

[3] Koga S, Morris S, Ogawa S, Liao H, Bilezikian JP, Chen G, Thompson WJ, Ashikaga T, Brett J, Stern DM, Pinsky DJ. TNF modulates endothelial properties by decreasing cAMP. Am J Physiol (Cell Physiol 37) 1995;268:C1104–13.

[4] Schafer AL, Gimbrone MA, Handin RI. Regulation of endothelial cell function by cyclic nucleotides. In: Jaffe EA, editor. Biology of endothelial cells. Boston: Martinus Nijhoff, 1984. p. 248–58.

[5] Ogawa S, Koga S, Kuwabara K, Brett J, Morrow B, Morris S, Bilezikian J, Silverstein S, Stern D. Hypoxia-induced increased permeability of endothelial monolayers occurs through lowering of cellular cyclic AMP levels. Am J Physiol 1992;262:C546–54.

[6] Stelzner T, Weil J, O'Brien R. Role of cyclic adenosine monophosphate in the induction of endothelial barrier properties. J Cell Physiol 1989;139:157–66.

[7] Conti M, Nemoz G, Sette S, Vicini E. Recent progress in understanding the hormonal regulation of phosphodiesterases. Endocr Rev 1995;16:1–20.

[8] Thompson WJ. Cyclic nucleotide phosphodiesterases: pharmacology, biochemistry and function. In: Taylor CW, editor. International encyclopedia of pharmacology and therapeutics. Oxford: Pergamon Press, 1993. Chap. 12, p. 287–313.

[9] Torphy TJ, Undem BJ. Phosphodiesterase inhibitors: new opportunities for the treatment of asthma. Thorax 1991;46:512–23.

[10] Beavo JA. Cyclic nucleotide phosphodiesterases: functional implications of multiple isoforms. Physiol Rev 1995;75:725–48.

[11] Haynes Jr. J, Kithas PA, Taylor AE, Strada SJ. Selective inhibition of cGMP-inhibitable cAMP phosphodiesterase decreases pulmonary vasoreactivity. Am J Physiol 1991;261:H487–92.

[12] Haynes Jr. J, Killilea DW, Peterson PD, Thompson WJ. Erythro-9-(2-hydroxy-3-nonyl)adenine (EHNA) inhibits cGMP-stimulated phosphodiesterase (PDE 2) to reverse hypoxic pulmonary vasoconstriction in the perfused rat lung. J Pharmacol Exp Ther 1996;276:752–7.

[13] Cohen AH, Hanson K, Morris K, Fouty B, McMurty IF, Clarke W, Rodman DM. Inhibition of cyclic 3′-5′-guanosine monophosphate-specific phosphodiesterase selectively vasodilates the pulmonary circulation in chemically hypoxic rats. J Clin Invest 1996;97:172–9.

[14] Souness JE, Scott LC. The specificity of rolipram actions on eosinophil cyclic AMP-specific phosphodiesterase. Biochem J 1993;291:389–95.

[15] Semmler J, Wachtel H, Endres S. The specific type IV phosphodiesterase inhibitor rolipram suppresses tumor necrosis factor-α production by human mononuclear cells. Int J Immunopharmacol 1993;15:409–13.

[16] Minnear F, Johnson A, Malik A. ß-Adrenergic modulation of pulmonary transvascular fluid and protein exchange. J Appl Physiol 1987;60:266–74.

[17] Seibert AS, Thompson WJ, Taylor AE, Wilborn WH, Barnard JW, Haynes JL. Increases in cyclic AMP reverse ischemia/reperfusion injury in the isolated rat lung. J Appl Physiol 1992;72:389–95.

[18] Farrukh IS, Gurtner GH, Michael JR. Pharmacological modification of pulmonary vascular injury: possible role of cyclic AMP. J Appl Physiol 1987;62:47–54.
[19] Kelly JJ, Moore TM, Babal P, Diwan AH, Stevens T, Thompson WJ. Pulmonary microvascular and macrovascular endothelial cells: differential regulation of Ca^{2+} and permeability. Am J Physiol (Lung Cell Mol Physiol 18) 1998;274:L810–9.
[20] Stevens T, Nakahashi Y, Cornfield DN, McMurtry IF, Cooper DMF, Rodman DM. Ca^{2+}-inhibitable adenylyl cyclase modulates pulmonary artery endothelial cell cyclic AMP content and barrier function. Proc Natl Acad Sci USA 1995;92:2696–700.
[21] Adkins WK, Barnard JW, May S, Siebert AF, Haynes JL, Allison RA, Taylor AE. Compounds that increase cyclic AMP prevent ischemia/reperfusion pulmonary capillary injury. J Appl Physiol 1992;72:492–7.
[22] Kennedy TP, Michael JR, Hoidal JR, Hasty D, Sciuto AM, Hopkins C, Lazar R, Bysani GK, Tolley E, Gurtner GH. Dibutyryl cAMP, aminophylline, and β-adrenergic agonists protect against pulmonary edema caused by phosgene. J Appl Physiol 1989;67:2542–52.
[23] Kobayashi H, Kobayashi T, Fukushima M. Effects of dibutyryl cAMP on pulmonary air embolism-induced lung injury in awake sheep. J Appl Physiol 1987;63:2201–7.
[24] Turner CR, Esser KM, Wheeldon EB. Therapeutic intervention in a rat model of ARDS: IV. Phosphodiesterase IV inhibition. Circ Shock 1993;39:237–45.
[25] Noel PE, Fletcher JR, Thompson WJ. Rolipram and isoproterenol reverse platelet activating factor (PAF)-induced increases in pulmonary microvascular permeability and resistance. J Surg Res 1995;59:159–64.
[26] Mizus I, Summer W, Farrukh I, Michael JR, Gurtner GH. Isoproterenol or aminophylline attenuate pulmonary edema after acid lung injury. Am Rev Respir Dis 1985;131:256–9.
[27] Ortiz JL, Cortijo J, Vallies JM, Morcillo EJ. Rolipram inhibits PAF-induced airway microvascular leakage in guinea-pig: a comparison with milrinone and theophylline. Fund Clin Pharmacol 1992;6:247–9.
[28] Thompson WJ, Danthuluri S, Strada SJ. Rolipram (ROL)-sensitive cyclic nucleotide (CN) phosphodiesterase (PDE) isozyme regulates cyclic AMP metabolism in pulmonary microvascular endothelial cells (PMVEC). FASEB J 1993;7:3127.
[29] Thompson WJ, Epstein PM, Strada SJ. Assay of cyclic nucleotide phosphodiesterase and resolution of multiple molecular forms of the enzyme. Adv Cyclic Nucleotide Res 1979;10:69–92.
[30] Whalin ME, Garrett Jr. ML, Thompson WJ, Strada SJ. Correlation of cell-free brain cyclic nucleotide phosphodiesterase activities to cyclic AMP decay in intact brain slices. Second Messengers Phosphoproteins 1989;12:311–25.
[31] Shakur Y, Wilson M, Pooley L, Lobban M, Griffiths SL, Campbell AM, Beattie J, Daly C, Houslay MD. Identification and characterization of the type-IVA cyclic AMP-specific phosphodiesterase RD1 as a membrane-bound protein expressed in cerebellum. Biochem J 1995;306:801–9.
[32] Bolger GB, Erdogan S, Jones RE, Loughney K, Scotland G, Hoffmann R, Wilkinson I, Farrell C, Houslay MD. Characterization of five different proteins produced by alternatively spliced mRNAse from the human cAMP-specific phosphodiesterase PDE4D gene. Biochem J 1997;328:539–48.
[33] Francis SH, Colbran JL, McAllister-Lucas LM, Corbin JD. Zinc interactions and conserved motifs of the cGMP-binding cGMP-specific phosphodiesterase suggest that it is a zinc hydrolase. J Biol Chem 1994;269:22477–80.
[34] Stevens T, Brough GH, Moore T, Babal P, Thompson WJ. Endothelial cells. In: Gerlack P, Taylor AE, editors. Methods in pulmonary research: a practical approach guide from the publisher. Basel: Birkhauser, 1997. p. 403–26.
[35] Magee JC, Stone AE, Oldam KT, Guice KS. Isolation, culture and characterization of rat lung microvascular endothelial cells. Am J Physiol 1994;267:L433–41.
[36] Reynolds PD, Strada SJ, Thompson WJ. Utilization of a new prelabeling technique to measure cyclic GMP accumulation in rat pulmonary microvascular endothelial cells. Life Sci 1997;60:909–18.
[37] Bradford MM. A rapid and sensitive method for the quantitation of microgram quantities of protein utilizing the principle of protein-dye binding. Anal Biochem 1972;72:660–72.
[38] Ashikaga T, Strada SJ, Thompson WJ. Altered expression of cyclic nucleotide phosphodiesterase isozymes during culture of aortic endothelial cells. Biochem Pharmacol 1997;54:1071–9.
[39] Lugnier C, Schini VB. Characterization of cyclic nucleotide phosphodiesterases from cultured bovine aortic endothelial cells. Biochem Pharmacol 1990;39:75–84.
[40] Souness JE, Diocee BK, Martin W, Moore SA. Pig aortic endothelial cell cyclic nucleotide phosphodiesterase. Biochem J 1990;266:127–32.
[41] Kishi Y, Ashikaga T, Numano F. Phosphodiesterases in vascular endothelial cells. Adv Second Messenger Phosphoprotein Res 1992;25:201–13.
[42] Iona S, Cuomo M, Bushnik T, Naro F, Sette S, Hess M, Shelton ER, Conti M. Characterization of the rolipram-sensitive, cyclic AMP-specific phosphodiesterases: identification and differential expression of immunologically distinct forms in the rat brain. Mol Pharmacol 1998;53:23–32.
[43] Livi GP, Kmetz P, McHale MM, Cieslinski LB, Sathe GM, Taylor DP, Davis RL, Torphy TJ, Balcarek JM. Cloning and expression of cDNA for a human low-K_m, rolipram-sensitive cyclic AMP phosphodiesterase. Mol Cell Biol 1990;10:2678–86.
[44] Houslay MD, Sullivan M, Bolger GB. The multienzyme PDE4 cyclic adenosine monophosphate-specific phosphodiesterase family: intracellular targeting, regulation, and selective inhibition by compounds exerting anti-inflammatory and antidepressant actions. Adv Pharmacol 1998;44:225–342.
[45] Barnette MS, Grous M, Cieslinski LB, Burman M, Christensen SB, Torphy TJ. Inhibitors of phosphodiesterase IV (PDE IV) increase acid secretion in rabbit isolated gastric glands: correlation between function and interaction with a high-affinity rolipram binding site. J Pharmacol Exp Ther 1995;273:1396–402.
[46] Owens RJ, Catterall C, Batty D, Jappy J, Russell A, Smith B, O'Connell J, Perry MJ. Human phosphodiesterase 4A: characterization of full-length and truncated enzymes expressed in COS cells. Biochem J 1997;326:53–60.
[47] Kostic MM, Erdogan S, Rena G, Borchert G, Hoch B, Bartel S, Scotland G, Huston E, Houslay MD, Krause E-G. Altered expression of PDE1 and PDE4 cyclic nucleotide phosphodiesterase isoforms in 7-oxo-prostacyclin-preconditioned rat heart. J Mol Cell Cardiol 1997;29:3135–46.
[48] Seid JM, MacNeil S, Tomlinson S. Calcium, calmodulin and the production of prostacyclin by cultured vascular endothelial cells. Biosci Rep 1983;3:1007–15.
[49] Suttorp N, Weber U, Welsch T, Schudt C. Role of phosphodiesterases in the regulation of endothelial permeability *in vitro*. J Clin Invest 1993;91:1421–8.